H14-162
REPRESENTATIVENESS OF URBAN MONITORING STATIONS

Jose Luis Santiago[1], Fernando Martín[1] and Alberto Martilli[1]

[1]Atmospheric Pollution Division, Environmental Department, CIEMAT, Spain.

Abstract: Measurements of urban monitoring stations have a limited spatial representativeness due to the complex urban meteorology. In this work, a methodology based on a set of RANS-CFD simulations for different wind directions is developed in order to analyse the spatial representativeness of urban monitoring stations and to complement the experimental measurements. Results show that average pollutant concentration can vary up to a factor of 3-4 within a distance of few tens of metres around the urban station.

Key words: Urban air quality, stations representativeness, RANS-CFD model, FAIRMODE.

INTRODUCTION

Urban air quality assessment is an important part of urban air quality management. This task is usually based on a network of urban monitoring stations. However, the interaction of urban morphology with atmospheric processes induces a complex flow field and produces pollutant concentration patterns with strong spatial heterogeneities inside the urban canopy layer. For this reason the spatial representativeness of point measurements is very limited and not even the densest monitoring network can capture this heterogeneity. Increase the number of stations to catch the behaviour of these heterogeneities is very expensive and often not possible in practice. In this work we propose to use RANS-CFD models to estimate the spatial representativeness of the urban air quality stations and to complement the experimental data obtained from them. These models resolve explicitly (resolution ~ m) the flow and pollutant dispersion around urban obstacles (building, trees,...) on spatial domains of several hundreds of meters. Their main disadvantage is the computational time that prevents unsteady simulations for large time periods. In order to overcome this problem, a methodology has been developed based on a set of steady RANS simulations for different inlet wind directions and several simple assumptions (non-reactive pollutants, negligible thermal effects,...). This methodology has been applied to zones of real cities in Spain. Results of this study indicate that pollutant concentration can vary up to a factor 3-4 within a distance of few tens of meters from the station in dense urban centres. Another advantage of this methodology is that it can be easily used also to evaluate strategies to improve air quality by testing different emissions scenarios.

METHODOLOGY

The objective of this methodology is to provide concentration maps with high spatial resolution (~ m) around the urban monitoring station. The methodology is based on CFD-RANS simulations for different wind directions. 16 wind directions are simulated (N, NNE, NE, etc.). The emissions are modelled with a line source inside each street and several tracers (one for each street) are emitted in each simulation.

Pollutant concentration is computed assuming that:
- Pollutants are considered non-reactive.
- Thermal effects are negligible in comparison with dynamical effects.
- Emissions inside each street at a selected hour are proportional to traffic at that hour.
- Tracer concentration at a certain hour only depends on emissions at that hour.

Taking into account these assumptions, a concentration proportional to the real one at time t is computed using ,

$$C_{\text{Real}}(t) \propto C_{\text{computed}}(Sector(t)) = \sum_i C_i(Sector(t)) \cdot \frac{L_i}{Vsource_i} \cdot N_i(t) \cdot \frac{1}{v_{in}(t)} \tag{1}$$

where,
- $C_{\text{Real}}(t)$ is the real concentration at time t.
- $Sector(t)$ is the wind direction sector at time t.
- i indicates the tracer emitted inside each street.
- $C_i(Sector(t))$ is the concentration computed for $Sector(t)$ for a given emission from street i and for a given inlet wind speed.
- L_i is the length of the street i.
- $Vsource_i$ is the volume of the row of computational cells where emission of the street i is located.
- $N_i(t)$ is the number of cars per unit time in street i.
- $v_{in}(t)$ is the inlet wind speed.

This methodology has difficulties in the estimation of concentration for low wind speed cases. For these cases, several assumptions are not fulfilled (e.g. thermal effects have more importance, concentration is not proportional to 1/v, etc).

Some considerations about equation (1) are the following:
- At each time t, we take the wind direction and use the CFD-RANS simulation corresponding to this wind sector. Only one CFD-RANS simulation is made for each wind direction.
- The factor $1/v_{in}(t)$ is used to modulate the modelled concentration in the case of the real inlet wind speed was different to the inlet wind speed used in the CFD simulations.
- The factor $\dfrac{L_i}{Vsource_i} \cdot N_i(t)$ is used to take into account the different emissions inside each street (CFD simulations are made using the same emission for each tracer).

More details about the methodology are shown in Parra, M.A. et al. (2010) and Santiago, J.L. et al. (2010).

APLICATION TO REAL CASES

A traffic monitoring station inside a square in Pamplona (Spain)
The methodology presented above has been applied to a square in Pamplona, a medium-size city of Spain. This square is surrounded by 15 m-high buildings. CFD simulations were based on Reynolds-averaged Navier-Stokes (RANS) equations. The turbulent closure used was standard k-ε. The tracers were simulated by means of a transport equation for passive scalar (Santiago, J.L. et al, 2007; Parra, M.A. et al., 2010). An irregular computational mesh with $3.5 \cdot 10^6$ cells approximately was used. The cell size was smaller close to buildings. We have a resolution of 2 m in X- and Y-direction and 1.5 m in Z-direction close to the buildings. Symmetry boundary conditions were used at the top and standard wall functions at solid boundaries (buildings and ground). Figure 1 shows the real geometry, the modelled geometry and a detail of the computational mesh. Simulations for 16 wind directions (one for each wind sector: N, NNE, NE, etc.) were performed.
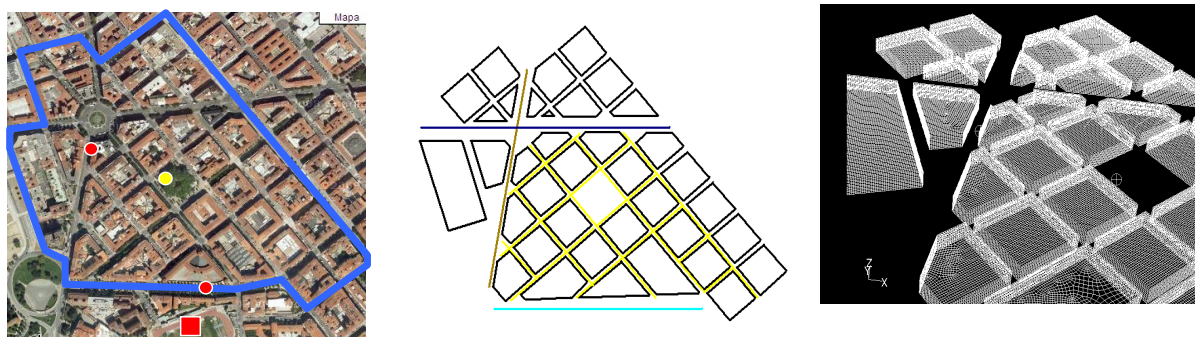

Figure 1. Left: Plan view of real geometry (dots are the locations of passive samplers, yellow dots the urban monitoring station and the quare is meteorological tower), Center: Modeled geometry (Color lines are locations of different traffic emissions). Right: Detail of the 3D computational mesh.

An evaluation of the results of the methodology was performed by comparing with experimental measurements (Santiago, J.L. et al., 2008). The time period of January and February 2007 was chosen because pollutants are little affected by atmospheric chemistry in winter (Sillman, S., 1999; Atkinson, R., 2000). Temporal evolution of hourly mean concentration of NOx and PM10 from the monitoring station were compared. A suitable agreement is observed. The highest differences are for cases where wind speed is very low.

Averaged tracer concentration maps for the time period of January and February 2007 were computed by applying weighted average for the simulations done for every wind sectors taking into account the wind speeds and directions frequencies occurred during the studied period. Note that the concentration is inversely proportional to wind speed. Meteorological conditions are computed for the time period January - February 2007 and from 8h to 20h of each day (when the largest part of the emissions are released). In figure 2 (left), the computed mean concentration (normalized by concentration at station location) is shown in the square, where the urban air quality station is located. Strong spatial variability in the pollutant concentration is modelled in this area. There can be differences larger than a factor 3, between concentrations in some streets and concentrations in the square. The white and grey colours represent where concentrations are within 20% of the concentration at the monitoring station, and can be considered as the representativeness area (RA) of the urban air quality station. The RA has a donut shape covering a portion of the square and small areas in few streets. Hypothetical locations of the new monitoring stations can be also evaluated based on these results, in order to choose the locations with largest RA, or to decide the number of stations needed to characterize air quality. For example, positions in another zone of the square and in a nearby street are considered (Figure 2, center and right). It can be observed that the spatial extension of the RA is strongly dependent on the position of the station. In this case, the location in the street seems to be more representative of the air pollution in the area than the square locations. In particular, concentration in the streets is quite homogeneous, while largest gradients are present in the square. If the aim of the study is to estimate exposure, this information should be

completed with people density (and residence time of the people in the different areas of the city), in order to choose the monitoring location which is not only representative of the largest area, but of what people breath.
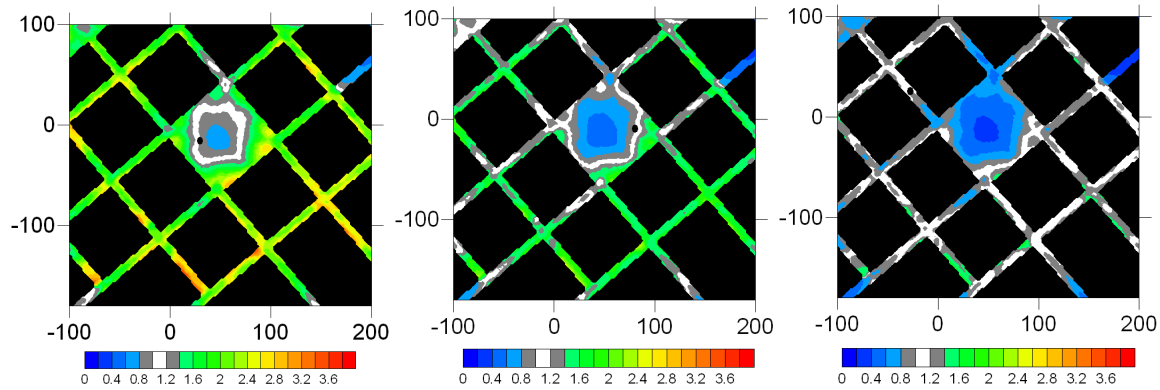

Figure 2. Mean concentration map normalized by concentration at station location (black dot). Left: Present location of the urban quality station. Center: Hypothetical location of urban AQ station in other square corner. Right: Hypothetical location of urban AQ station in a street close to the square. The axis units are m.

A traffic monitoring station close to an urban park in Madrid (Spain)
The proposed methodology was also applied to investigate the representativeness of a traffic station of the Madrid City located in an area with intense road traffic and close to an urban green area (Fig. 3).

The dimensions of studied zone are 700 m x 800 m around the air quality station. The buildings of this area have different heights. Tallest building is 90m high approximately but most of the others buildings have a height between 18m and 24m. An irregular mesh of $3 \cdot 10^6$ computational cells with a resolution of about 1m-3m close to the buildings is used. A test about grid independence of results was made, and it has shown that this resolution is acceptable.

Some additional considerations were taken into account in these simulations respect to the Pamplona case:
1. The dynamic effects of vegetation were included assuming the trees as a porous medium.
2. Background concentrations from urban background stations were added to the results of the simulations as they only represent the local traffic impact.
3. 16 wind sector cases with wind speed higher than 2 m s^{-1} at 10m-height were simulated and the same methodology than Pamplona was used. Meteorological data from the AEMET (Spanish Meteorological Agency) of a near station were used.
4. In the case of weak winds (lower than 2 m s^{-1}) the methodology was modified. For these cases, thermal effects are not negligible. For these cases we assume that the pollutant concentration is independent of wind direction and it is modelled depending on traffic intensity and mixing height along the day. This assumption allows to take into account indirectly the thermal effects. A simple parameterization of mixing height is considered. From 1h to 8h we considered that it was 100m, from 15h to 18h was 1500m and for the other hours a linear change between these values was assumed. In future works these cases have to be investigated in depth.
5. Days with Saharan dust outbreak episodes were removed in the computation of PM10 concentration.
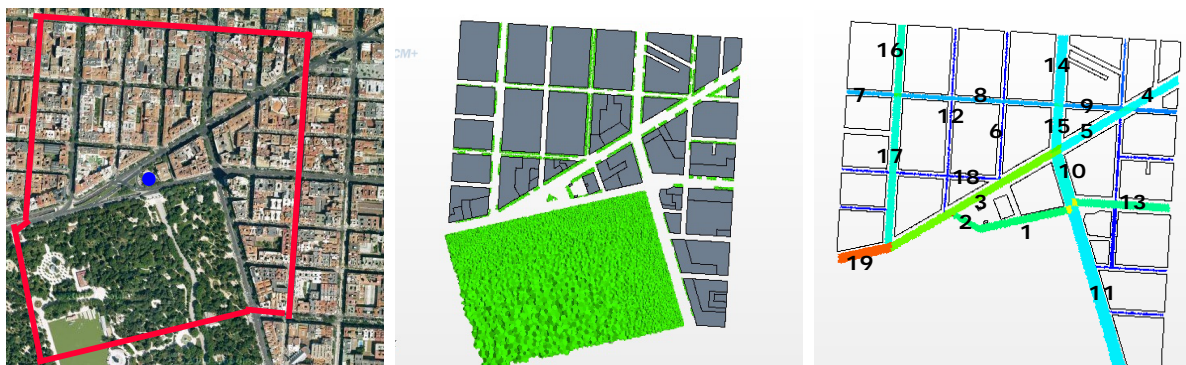

Figure 3. Left: Aerial picture of the domain (red line) including the location of the air quality station. Center: Modeled geometry of the domain including street and park vegetation. Right: relative traffic intensity in the main streets of the domain (red and blues shows maxima and minima intensities (respectively).

The simulated period was January-May 2011. Comparison with observed data in the air quality stations were carried out for hourly data for NO$_2$ and PM10 and also for daily mean concentrations of PM10 (Figures 4 and 5). The results were quite good showing the simulated data fit well the observations for both pollutants.
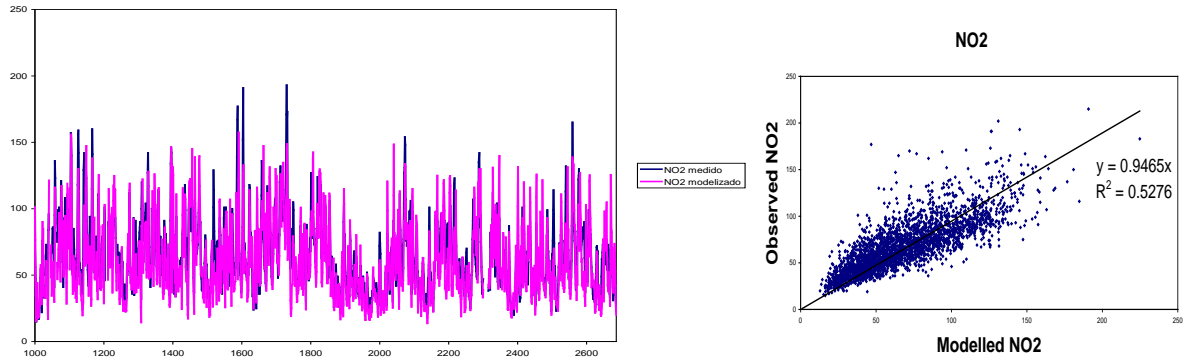
Figure 4. Comparison between modeled and measured hourly NO₂ concentrations. Left: Time series. Right: Scatter-plot.
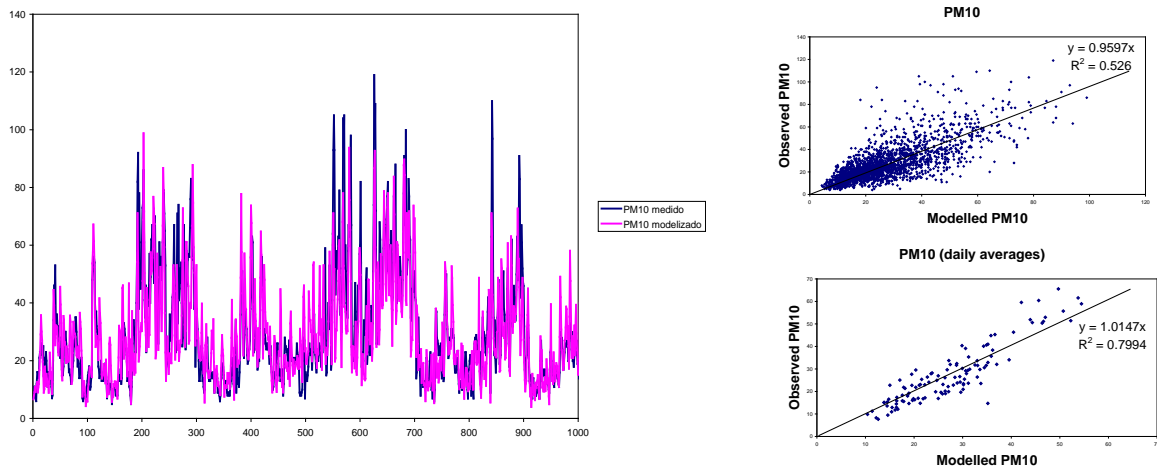

Figure 5. Comparison between modeled and measured PM10 concentrations. Left: Time series of hourly concentrations. Upper right: Scatter-plot of hourly data. Lower right: Scatter plot of daily averaged data.

Averaged NO2 and PM10 concentration maps for the time period of January-May 2011 were computed by applying weighted average for the simulations done for every wind sectors taking into account the wind speeds and directions frequencies occurred during the studied period and the dependence of the concentrations with the wind speed (see equation (1)) for wind speed higher than 2 m s^{-1}. For weak wind speed a dependency proportional to traffic intensity and 1/mixing height$^{0.3}$ was assumed. The dependency with mixing height was fitted from experimental data. This assumption should be investigated in future works studying in depth urban thermal effects.

The averaged normalized maps for both pollutants are pretty similar showing a representativeness area (grey colour in figures 6) extending along the sidewalk close to the northern border of the park, a relatively small area around the station and some streets of less traffic intensity. There is a very remarkable variability in the pollutant concentrations in the main streets (up to a factor of 2). The representativeness criterion was the same used for the Pamplona case.
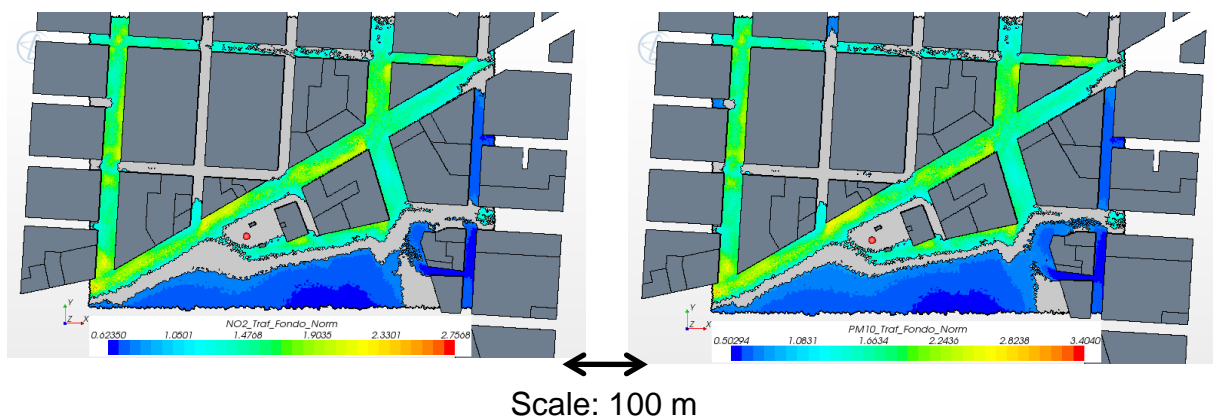

Scale: 100 m

Figure 6. Mean concentration map normalized by concentration at station location (red dot) for NO₂ (left) and PM10 (right). Grey shows the area with concentrations into ±20% around the station concentration.

In order to check the representativeness for exceedances of the hourly and daily limit values for NO_2 and PM10, respectively, maps of 99.8 percentile of hourly data of NO_2 and 90.4 percentile of daily data of PM10 were computed (Fig. 7). The representativeness area (grey colour) is almost the same than in the long-term average cases (Fig. 6). In the case of NO_2, the representativeness area is larger including part of the urban park. The gradients of concentrations are clearly higher than in the long-range averages cases.
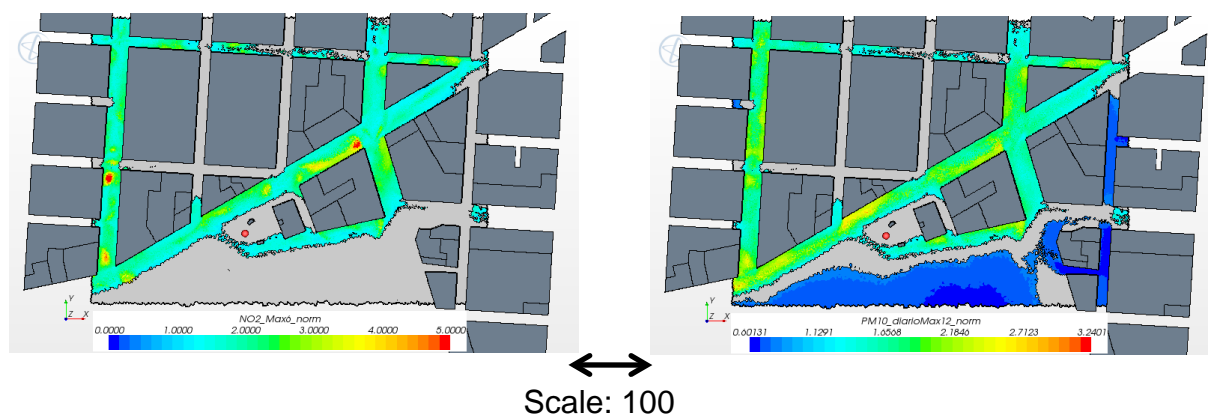

Scale: 100

Figure 7. Concentration map normalized by concentration at station location (red dot) for 99.8 percentile of hourly data of NO_2 (left) and 90.4 percentile of daily data of PM10 (right). Grey shows the area with concentrations into ±20% around the station concentration.

CONCLUSIONS

These results show a suitable performance of the CFD-RANS simulations when compared with the observations. It gives confidence to use CFD-RANS simulations to estimate the distribution of pollutants in the streets near the air quality stations and then, to estimate the spatial representativeness of the air quality stations by analyzing how similar is the station concentration to that of its surroundings.

The two cases shown in this paper corresponding to two stations of two Spanish cities demonstrate that their spatial representativeness seems to not meet completely the requirements of the Air Quality Directive (EC/2008/50) stating that "…a sampling point must be sited in such a way that the air sampled is representative of air quality for a street segment no less than 100 m length at traffic-orientated sites…". More importantly, due to the strong heterogeneities in the pollutant concentration patterns in the streets it is practically impossible to find measurements location that fulfils the Directive's requirement. This is due to the complex flow over the streets. In our opinion, the simple rule stated in the Directive must be revised. This should include a better definition of representativeness (should be based only on spatial extension or also on people density?), and should recommend the use of CFD models to decide the best location.

REFERENCES

Atkinson, R., 2000: Atmospheric chemistry of VOCs and NOx. Atmos. Environ., **34**, 2063-2101.

Parra, M. A., Elustondo, D., Bermejo, R., Santiamaría, J. M., 2009: Ambient air levels of volatile organic compounds (VOC) and nitrogen dioxide (NO2) in a medium size city in Northern Spain. Sci. Total Environ., **407**, 999-1009.

Parra, M. A., Santiago, J. L., Martín, F., Martilli, A., Santamaría, J. M., 2010: A methodology to urban air quality assessment during large time periods of winter using computational fluid dynamic models. Atmos. Environ., **44**, 2089-2097.

Santiago, J. L., Martilli, A., Martín, F., 2007: CFD simulation of airflow over a regular array of cubes. Part I: three-dimensional simulation of the flow and validation with wind tunnel measurements. Boundary-Layer Meteorol., **122**, 609-634.

Santiago J.L., M.A. Parra, F. Martín and J.M. Santamaría (2008). Numerical and experimental study of air quality in the Pamplona downtown (Navarra, Spain). Proceedings of HARMO12. Cavtat (Croatia).

Santiago J. L., M. A. Parra, A. Martilli, F. Martín, J. M. Santamaría (2010). Analysis of spatial representativeness of urban monitoring stations using steady CFD-RANS simulations. Proceedings of 9th Symposium on the Urban Environment. Keystone. Colorado. USA

Sillman, S., 1999: The relation between ozone, NOx and hydrocarbons in urban and polluted rural environments. Atmos. Environ., **33**, 1821-1845.